Phase Transitions in Sphere-Forming Polystyrene-*block*-polyisoprene-*block*-polystyrene Copolymer and Its Blends with Homopolymer

Soobum Choi, Kyung Min Lee, and Chang Dae Han*

Department of Polymer Engineering, The University of Akron, Akron, Ohio 44325

Norihiro Sota and Takeji Hashimoto*

Department of Polymer Chemistry, Graduate School of Engineering, Kyoto University, Kyoto 606-8501, Japan

Received May 3, 2002

ABSTRACT: Phase transitions in sphere-forming polystyrene-*block*-polyisoprene-*block*-polystyrene (SIS triblock) copolymer and its blends with polystyrene (PS) were investigated using oscillatory shear rheometry, transmission electron microscopy, and small-angle X-ray scattering (SAXS). For the investigation, a commercial grade of high-molecular-weight SIS triblock copolymer (Vector 4113, Dexco Polymers) and a low-molecular-weight SIS triblock copolymer (SIS-100) synthesized in our laboratory were used. It is found from oscillatory shear rheometry and SAXS that both Vector 4113 and SIS-100 undergo order−disorder transition (ODT) having a characteristic feature of lattice disordering/ordering transition (LDOT) of spheres, giving rise to a phase consisting of micelles with short-range liquidlike order at thermal equilibrium above ODT and demicellization/micellization transition (DMT), as a pseudo phase transition, giving rise to a micelle-free phase with only thermal composition fluctuations. The LDOT temperature (T_{LDOT}) of Vector 4113 is found to be ca. 205 °C, and the DMT temperature (T_{DMT}) is much higher than 220 °C, the highest experimental temperature employed to avoid thermal degradation/cross-linking reactions. The addition of various amounts of low-molecular-weight PS enabled us to estimate, via extrapolation, the T_{DMT} of Vector 4113 to be ca. 260 °C. On the other hand, SIS-100 is found to have T_{LDOT} of 85 °C and T_{DMT} of 105 °C. Transmission electron microscopy confirmed the existence of disordered micelles in both Vector 4113 and SIS-100 between T_{LDOT} and T_{DMT}. Phase diagrams for (SIS-100)/PS blends were constructed using T_{LDOT}, T_{DMT}, and cloud point measurements.

1. Introduction

A number of research groups have investigated phase transitions in block copolymers, but there are too many papers to cite all of them here. The interested readers are referred to a recent review paper.[1] It is well established theoretically that phase transitions in block copolymers are intimately related to their microdomain structures, which in turn depend on block composition.[2,3] The majority of the past experimental studies dealt with phase transitions in compositionally symmetric or nearly symmetric AB-type diblock or ABA-type triblock copolymers having lamellar or hexagonally packed cylindrical microdomain structures, and much fewer studies[4−12] dealt with phase transitions in highly asymmetric block copolymers having spherical microdomains. In a series of our recent papers,[8−11] we found that the phase transition in sphere-forming block copolymers has a feature different from that in lamella-forming block copolymers as described below.

Specifically, using small-angle X-ray scattering (SAXS), oscillatory shear rheometry, and transmission electron microscopy (TEM), we have shown[11] that a sphere-forming polystyrene-*block*-polyisoprene (SI diblock) copolymer undergoes, during heating, lattice disordering transition transforming spheres in body-centered-cubic (bcc) lattice into spheres with short-range liquidlike order (disordered micelles or spheres). This is followed by demicellization transition transforming into the micelle-free state having thermal composition fluctuations (which will be referred to hereafter as homogeneous phase), upon further heating. During cooling, the highly asymmetric SI diblock copolymer in the homogeneous state undergoes micellization transition forming disordered micelles and then lattice ordering transition transforming into spheres in bcc lattice. We have referred to the two transitions as "lattice disordering/ordering transition" (LDOT) and "demicellization/micellization transition" (DMT) in highly asymmetric, sphere-forming block copolymers. We note that DMT is a pseudo phase transition, but not a true phase transition from a rigorous thermodynamic point of view, in the sense that it does not occur in an effectively infinite system and it does not occur at a precise transition temperature with infinite sharpness, while LDOT is much closer to a true phase transition than DMT. Both LDOT and DMT are thermally reversible transitions. The micelles are a thermodynamically stable phase, which exist even at temperatures far above the glass transition temperatures of the micelles and their matrix. The formation of micelles is a kind of ordering process, and disappearance of micelles is a kind of disordering process since the entropy of the system associated with the formation of micelles decreases while the entropy of the system associated with the disappearance of micelles increases.[13] On the other hand, in compositionally symmetric or nearly symmetric block copolymers, lamellar microdomains with long-range order transform directly into the micelle-free homogeneous state, in which component blocks are molecularly mixed, with thermal composition fluctuations. This phase transformation is referred to as order−disorder transition (ODT) in the theory of Fredrickson and Helfand.[15] Thus, in

10.1021/ma020684q CCC: $25.00
Published on Web 01/11/2003

symmetric or nearly symmetric diblock copolymers LDOT and DMT essentially degenerate into a single transition, ODT.

We believe that it is very important to distinguish the disordered state with micelles from that without micelles. The disordered state with micelles can also be regarded as a thermodynamically homogeneous phase with composition fluctuations. However, it is very important to recognize that the composition fluctuations in the disordered state with micelles are different from those without micelles; namely, the composition fluctuations in the disordered state *with micelles* cannot be dealt with using the Fredrickson−Helfand theory.[15] In the Appendix we have clarified some of the statements that appeared in our previous paper,[11] which might be misinterpreted.

Earlier, Hashimoto et al.,[14] Kinning et al.,[16,17] and Winey et al.[18] reported that lattice disordering transition took place in binary mixtures consisting of an SI or polystyrene-*block*-polybutadiene diblock copolymer and homopolystyrene. They observed, via SAXS and TEM, the formation of disordered micelles, upon increase in temperature or increase in homopolymer volume fraction, from ordered morphologies (or ordered micelles) before the onset of the dissolution of micelles into the homogeneous state. They emphasized that both spatially ordered and spatially disordered micelles are microphase-separated; thus, the lattice disordering transition between the ordered morphologies and the disordered micelles is *not* the ODT as defined for lamella- or cylinder-forming block copolymer, i.e., ODT between the ordered phase and the micelle-free homogeneous phase. The lattice disordering transition defined by Hashimoto et al.[14] and Winey et al.[18] is essentially the same as the LDOT defined here.

Very recently, Dormidontova and Lodge[19] extended Semenov's strong-segregation theory[20,21] for highly asymmetric block copolymers. Interestingly, they were able to confirm the experimental results[8,9,11] of the existence of disordered micelles in sphere-forming diblock copolymers at elevated temperatures, while previous mean-field calculations could not.[2,3,22,23] Dormidontova and Lodge defined that disordered micelles are part of the disordered phase. We consider that this definition is acceptable as long as the disordered phase is clearly defined and is consistent with the definition of LDOT. However, we believe that LDOT defines more clearly than ODT in describing the nature of the transition and structures of systems below and above the transition for highly asymmetric block copolymers. The mean-field approach employed by Dormidontova and Lodge has been successful in predicting the existence of the disordered micellar phase.

In a recent paper,[24] Lee et al. investigated thermal transitions in a sphere-forming polystyrene-*block*-polyisoprene-*block*-polystyrene (SIS triblock) copolymer (Vector 4113, Dexco Polymers). They concluded that the T_{ODT} of Vector 4113 is ca. 230 °C as determined from dynamic temperature ramp experiment at an angular frequency of 0.1 rad/s and SAXS. However, they did not mention whether Vector 4113 might have formed disordered micelles at temperatures above 230 °C. By adding a low-molecular-weight polystyrene (PS) to Vector 4113, Lee et al. observed that the T_{ODT} of Vector 4113/PS blends went through a minimum followed by a maximum as the amount of added PS was increased. They attributed the observed dependence of T_{ODT} on blend composition to "chain stretching".

Very recently, we also investigated thermal transitions in Vector 4113. Owing to the very high molecular weight of Vector 4113, it was not possible for us to determine its T_{DMT}. Therefore we synthesized a low-molecular-weight SIS triblock copolymer (SIS-100), which enabled us to determine both T_{LDOT} (85 °C) and T_{DMT} (105 °C). When a low-molecular-weight PS was added to SIS-100, we observed that both T_{LDOT} and T_{DMT} increased monotonically with increasing amount of added PS until reaching the binodal curve. Phase diagrams for (SIS-100)/ PS blends are constructed using T_{LDOT}, T_{DMT}, and cloud point measurements. In this paper we present the highlights of our findings.

2. Experimental Section

Materials. A commercial grade of sphere-forming SIS triblock copolymer (Vector 4113, Dexco Polymers Co.) was employed, and a low-molecular-weight SIS triblock copolymer was synthesized, via anionic polymerization, in our laboratory using a difunctional initiator. Also, two nearly monodisperse polystyrenes were synthesized, via anionic polymerization, in our laboratory.

(a) Synthesis of Nearly Monodisperse Polystyrene. Using anionic polymerization, we synthesized two homopolystyrenes (PS-1 and PS-2) having different molecular weights using *sec*-butyllithium (*sec*-BuLi) as initiator and cyclohexane as solvent. The polymerization was terminated by addition, via syringe, of a small amount of degassed methanol into the reactor. The solution was precipitated by addition of an excess amount of methanol. The precipitated polymer was filtered and dried first at room temperature for 3 days in a fume hood and then at 60 °C for 12 h in a vacuum oven.

(b) Synthesis of SIS Triblock Copolymer. There are two methods to synthesize SIS triblock copolymer having exactly the same average molecular weights for the two PS end blocks. One method is to first synthesize an SI diblock copolymer using a monofunctional initiator and then couple it to obtain an SIS triblock copolymer. It is a well-known fact that the SIS triblock copolymers synthesized by the coupling method contain about 20% of *uncoupled* SI diblock copolymer. Some commercial SIS triblock copolymers (Kraton series, Kraton Polymer Co.) are prepared using this method. The other method is to synthesize an SIS triblock copolymer by polymerizing isoprene and styrene monomers successively using a difunctional initiator. This method yields 100% SIS triblock copolymer. Some commercial SIS triblock copolymers (Vector series, Dexco Polymer Co.) are prepared by this method. We wish to mention that very few people, if any, have synthesized SIS triblock copolymers (ABA-type triblock copolymers in general) using sequential polymerization because it is practically impossible to synthesize, via sequential polymerization, compositionally symmetric SIS triblock copolymers having exactly the same molecular weight of the two PS end blocks; invariably, the average molecular weight of the last PS block will be different from that of the first PS block in sequential polymerization.

In the present study, we synthesized, via anionic polymerization, an SIS triblock copolymer (SIS-100) using a difunctional initiator. For this, we first prepared the difunctional initiator by purifying a precursor, 1,3-bis(phenylethenyl)-benzene (PEB) (yellowish liquid), which was received from Dow Chemical Co. Specifically, PEB was purified by first dissolving a crude, viscous PEB in *n*-hexane and then by passing repeatedly the PEB/*n*-hexane solution through a column packed with activated silica gel with sizes between 230 and 400 mesh (Selecto Scientific) until only one spot in TLC was detected. The purified PEB/*n*-hexane solution was distilled under a high vacuum. Earlier, Tung and Lo[25] purified PEB by recrystallization with methanol to obtain precursor in the crystal form, while Broske et al.[26] purified PEB by distillation under a high vacuum and obtained a clear viscous liquid as

Table 1. Summary of the Molecular Characteristics of the Polymers Investigated in This Study

sample code	M_n (g/mol)[a]	M_w/M_n[b]	w_{PS}[c]	f[d]
(a) SIS triblock copolymer				
vector 4113	1.44×10^5	1.06	0.153	0.13
SIS-100	1.09×10^5	1.05	0.083	0.07
(b) polystyrene				
PS-1	9×10^2	1.12	N.A.	N.A.
PS-2	1.3×10^3	1.12	N.A.	N.A.

[a] Number-average molecular weight (M_n) determined by membrane osmometry. [b] Polydispersity (M_w/M_n) determined by gel permeation chromatography. [c] Weight fraction of PS block (w_{PS}) determined by nuclear magnetic resonance spectroscopy. [d] Volume fraction of PS block (f) calculated at room temperature. Note that the value of f varies with temperature, because the temperature dependences of specific volumes of PS and PI are different.

precursor, and Lee[27] purified PEB by column chromatography and recrystallization with methanol and obtained precursor in the crystal form. Dilithium initiator (DLI) was prepared by reacting 2 mol of *sec*-BuLi with 1 mol of PEB in cyclohexane. The DLI thus obtained was analyzed, via proton nuclear magnetic resonance (^{1}H NMR) spectroscopy, to confirm the molecular structure and completeness of the addition reaction.

Pentamethyldiethylenetriamine (PMDETA) (Aldrich) needed to obtain narrow molecular weight polyisoprene (PI) was purified by vacuum distillation in the presence of calcium hydride. PMDETA with a mole ratio of 0.18/1 for *sec*-BuLi was added to the reactor using a syringe. The reactor was then purged with argon gas and heated, while stirring, to 55 °C using a water bath. When the temperature of the water bath reached about 55 °C, DLI and PMDETA were added to first polymerize the isoprene monomer. About 2 h after the addition of DLI, styrene monomer was added to the reactor. After the copolymerization of isoprene and styrene monomers for 1.5 h, a small amount of degassed methanol was added to terminate the living polymers, at which point the color of the solution changed from yellowish red to colorless. Then the reactor temperature was lowered to room temperature, and the solution was precipitated by addition of an excess amount of methanol. The precipitated polymer was filtered and dried at room temperature for 3 days in a fume hood and then at 60 °C for 12 h in a vacuum oven.

Characterization of the Polymers Synthesized. Membrane osmometry (Jupiter Instrument) was used to determine the number-average molecular weight (M_n) and gel permeation chromatography (GPC) (Waters) to determine the polydispersity index (M_w/M_n) of Vector 4113, SIS-100, and two polystyrenes (PS-1 and PS-2) synthesized in this study. Using ^{1}H NMR spectroscopy and GPC, we confirmed that both Vector 4113 and SIS-100 have 100% triblock. Table 1 gives a summary of sample codes and the molecular characteristics of the polymers employed in this study.

Sample Preparation. Samples were prepared by first dissolving a predetermined amount of Vector 4113, SIS-100, or its blends with homopolystyrene in toluene (10 wt % in solution) in the presence of 0.1 wt % antioxidant (Irganox 1010, Ciba-Geigy Group) and then slowly evaporating the solvent. The evaporation of solvent was carried out initially in a fume hood slowly at room temperature for 1 week, and the last trace of solvent was removed by drying the samples in a vacuum oven at an elevated temperature for varying periods, depending upon the block copolymer and its blends with homopolystyrene. The drying of the samples was continued until there was no further change in weight, and then the specimens were stored in a refrigerator. The details of the annealing temperature and the duration of annealing employed will be given when the experimental results of neat block copolymer, and its blends are presented.

Oscillatory Shear Rheometry. In this study, an Advanced Rheometric Expansion System (ARES, Rheometric Scientific) was used in the oscillatory mode with parallel plate fixtures (25 mm diameter). Dynamic frequency sweep experiments were conducted; i.e., the dynamic storage modulus (G') and dynamic loss modulus (G'') were measured as functions of angular frequency (ω) ranging from 0.01 to 100 rad/s at various temperatures during heating. The temperature increment in the frequency sweep experiment varied from 3 to 10 °C, and the specimen was kept at a constant temperature for 30−40 min before rheological measurements actually began. Data acquisition was accomplished with the aid of a microcomputer interfaced with the rheometer. The temperature control was satisfactory to within ±1 °C. For the rheological measurements, the strain was varied from 0.03 to 0.3 depending upon the measurement temperature, which was well within the linear viscoelastic range for the materials investigated. Dynamic temperature sweep experiments under isochronal conditions were also conducted; i.e., G' was measured at $\omega = 0.01$, 0.1, 1.0, or 2.0 rad/s during heating. All experiments were conducted under a nitrogen atmosphere to preclude oxidative degradation of the samples.

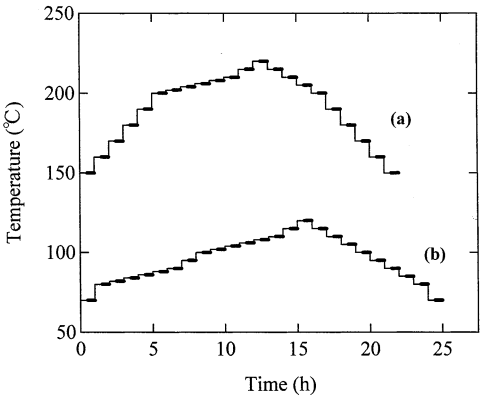

Figure 1. Schematic diagram describing the thermal histories of specimens employed for SAXS experiments: (a) Vector 4113 with 30 min preset time and 30 min exposure time and (b) SIS-100 with 30 min preset time and 30 min exposure time.

SAXS Experiment. SAXS experiments were conducted under a nitrogen atmosphere in the heating and cooling processes, using an apparatus described in detail elsewhere,[28,29] which consists of an 18 kW rotating-anode X-ray generator operated at 40 kV × 300 mA (MAC Science Co. Ltd., Yokohama, Japan), a graphite crystal for incident-beam monochromatization, a 1.5 m camera, and a one-dimensional position-sensitive proportional counter. The Cu Kα line (λ = 0.154 nm) was used. The SAXS profiles were measured as a function of temperature and were corrected for absorption, air scattering, slit height, and slit width smearing.[30] The absolute SAXS intensity was obtained using the nickel-foil method.[31] The temperature of the SAXS experiment was controlled using a specially constructed enclosure that was sealed by nitrogen gas. This temperature enclosure and controller enabled us to maintain the sample temperature to within ±0.002 °C. Figure 1 describes the thermal protocols of specimens employed for SAXS experiments. Namely, a specimen was exposed to the X-ray beam to measure SAXS profiles for the period indicated by each horizontal solid line (typically for 30 min) after holding for 30 min at each temperature increment during the heating process or at each temperature decrement during the cooling process.

Transmission Electron Microscopy (TEM). The morphology of the neat block copolymers was investigated via TEM. The ultrathin sectioning was performed by cryoultramicrotomy at −100 °C using a diamond knife, which was below the glass transition temperature (T_g = −68 °C) of PI to attain specimen rigidity, using a Reichert Ultracut S low-temperature sectioning system. A transmission electron microscope (JEM1200EX II, JEOL) operated at 120 kV was used to record the morphology of the specimens stained with osmium tetroxide vapor. The thermal histories of the specimens used for TEM experiments were as follows. For Vector 4113, a specimen was annealed at 150 °C for 3 days followed by rapid quenching in ice water or annealed at 210 °C for 10 h followed by rapid

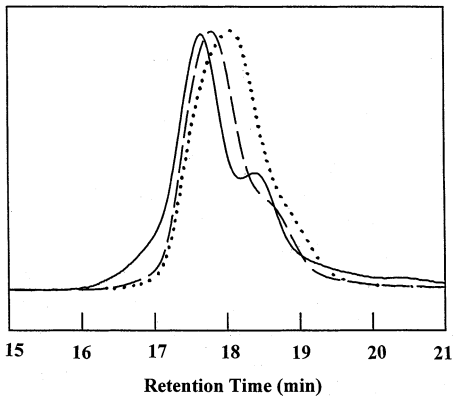

Figure 2. Effect of annealing condition on the GPC traces of Vector 4113: (· · ·) without annealing (i.e., as received); (– – –) after annealing 130 °C for 3 days in a vacuum oven; (—) after annealing at 130 °C for 3 days in a vacuum oven followed by heating at a rate of 1 °C/min to 260 °C in a differential scanning calorimeter.

quenching in ice water. For SIS-100, a specimen was annealed at 70 °C for 4 weeks followed by rapid quenching in ice water or annealed at 95 °C for 1 week followed by rapid quenching in ice water.

3. Results and Discussion

In this study we employed SAXS and both dynamic frequency sweep and isochronal dynamic temperature sweep experiments to determine phase transition temperatures of Vector 4113 and SIS-100. There were three precautions we had to take in conducting oscillatory shear flow experiments and SAXS study to obtain reproducible determination of phase transition temperatures of sphere-forming block copolymers, Vector 4113 and SIS-100. One was the angular frequency that was to be applied to a specimen when conducting isochronal dynamic temperature sweep experiment. The second precaution we had to take was to determine the highest measurement temperature for SAXS and oscillatory shear rheometry at and below which thermal degradation/cross-linking reactions of specimens would be considered negligible. The third precaution we had to take was to give adequate thermal treatment to the specimens prior to SAXS study and oscillatory shear measurement.

Figure 2 gives GPC traces of Vector 4113 specimens (i) without annealing (i.e., as received) (dotted line), (ii) after annealing at 130 °C for 3 days in a vacuum oven followed by rapid quenching in ice water (dashed line), and (iii) after annealing at 130 °C for 3 days in a vacuum oven and then heating to 260 °C at a rate of 1 °C /min in a differential scanning calorimeter (solid line), following the temperature protocol described in a paper of Lee et al.[24] It is seen in Figure 2 that the GPC trace of the specimen that was annealed first at 130 °C for 3 days and then heated to 260 °C at a rate of 1 °C /min, denoted by a solid line (—), has two peaks, while the as-received specimen has a single peak. Analysis of the GPC traces indicates that severe thermal degradation/cross-linking reactions took place when a Vector 4113 specimen had been annealed at 130 °C for 3 days followed by heating to 260 °C at a rate of 1 °C /min. This is manifested by a 20% increase in M_n (as determined by membrane osmometry) and a broadening of polydispersity index (as determined by GPC) from 1.16 to 1.21. The above observation guided us to conduct SAXS and rheological measurements at temperatures

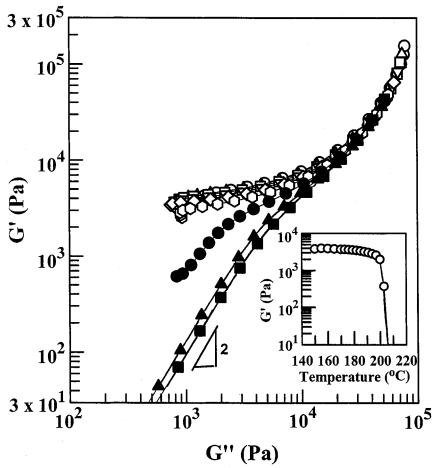

Figure 3. Plots of log G' vs log G'' for Vector 4113 at various temperatures: (○) 150, (△) 160, (□) 170, (▽) 180, (◇) 190, (⬡) 200, (●) 205, (▲) 210, and (■) 220 °C. The inset in the lower right corner gives the dependence of G' on temperature during the isochronal dynamic temperature sweep experiment at $\omega = 0.01$ rad/s in the heating cycle. The specimens were annealed at 130 °C for 3 days in a vacuum oven.

below which thermal degradation/cross-linking reactions may be regarded as being negligible. Previous study[32] suggests that SIS triblock copolymers begin to undergo serious thermal degradation/cross-linking reactions at ca. 220 °C.

Phase Transitions in Vector 4113. Figure 3 gives plots of log G' vs log G'' for Vector 4113 at various temperatures ranging from 150 to 220 °C, which were prepared from the dynamic frequency sweep experiments during heating. Also given in the inset of Figure 3 are the results of the isochronal dynamic temperature sweep experiment at $\omega = 0.01$ rad/s. Prior to the rheological measurements, the specimens were annealed at 130 °C for 3 days in a vacuum oven. It is seen in Figure 3 that the log G' vs log G'' plot makes a sudden shift downward at 205 °C with a slope close to 2 in the terminal region, another parallel shift downward at 210 °C, and a further parallel shift downward at 220 °C, the highest experimental temperature employed, above which significant thermal degradation/cross-linking reactions may take place. Following the rheological criterion of Han et al.,[33] we can conclude from Figure 3 that Vector 4113 has microdomain structures over the entire range of temperatures tested, because there is no threshold temperature at which the log G' vs log G'' plot becomes independent of temperature. On the other hand, the result of the isochronal dynamic temperature sweep experiment (the inset of Figure 3) shows a precipitous drop in G' at ca. 200 °C, which is close to 205 °C at which the log G' vs log G'' plot begins to show a slope of 2 in the terminal region. In our previous papers,[8,9,11] we have shown that for highly asymmetric, sphere-forming block copolymers a rapid drop in G' during isochronal dynamic temperature sweep experiments does not signify the onset of the ODT as found for lamella- or cylinder-forming block copolymers[34–36] but rather actually signifies the onset of LDOT.

Representative TEM images for Vector 4113 are given in Figure 4. We find that at 210 °C the ordered lattice of PS spheres initially observed at 150 °C (see Figure 4a) has already undergone large thermal distortions, and the system tends to exhibit disordered spheres (micelles)[8–11] (see Figure 4b), which will be elaborated on later (i.e., quantitatively) using the SAXS results

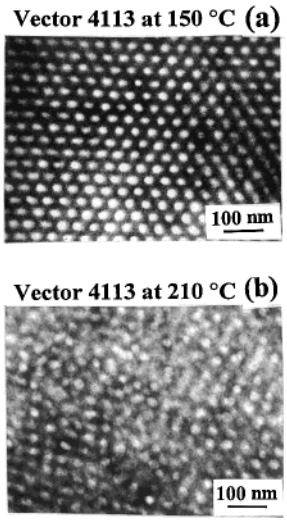

Figure 4. TEM images of Vector 4113: (a) after annealing at 150 °C for 3 days followed by rapid quenching in ice water; (b) after annealing at 210 °C for 10 h followed by rapid quenching in ice water.

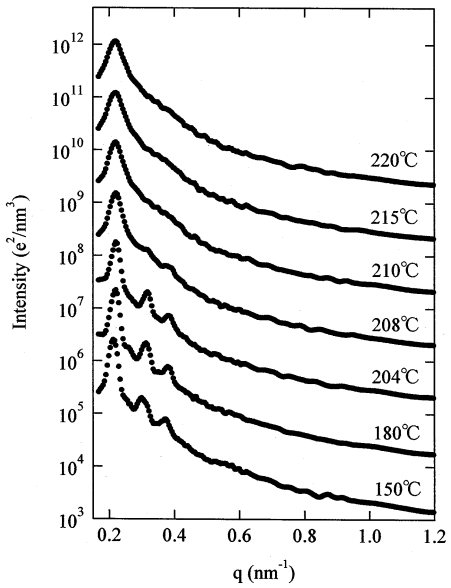

Figure 5. Temperature dependence of SAXS profiles for Vector 4113 in the heating process at various temperatures ranging from 150 to 220 °C. The intensities of the SAXS profiles at 150 °C shown at the bottom of this figure are actually measured values, and the intensities of other SAXS profiles have been shifted up by 1 decade relative to intensities immediately below.

shown in Figures 5 and 6. Note that 210 °C is above the temperature (ca. 200 °C) at which G' in the isochronal dynamic temperature sweep experiment begins to drop precipitously. Therefore, it is our view that 200 °C cannot be regarded as being the temperature above which the block copolymer attains a truly disordered state or the micelle-free homogeneous state having only thermally induced composition fluctuations. One may infer from the TEM image in Figure 4b coexistence of a more ordered region and a less ordered region, which is again more clearly and quantitatively presented by the SAXS results given in Figure 6. We note that the average diameter of the spherical microdomains is about 10.6 nm and the thickness of ultrathin section is 50−100 nm. In the TEM image shown in Figure 4a, which typically represents the ordered bcc phase, the microdomains are completely overlapped along the electron beam direction (i.e., along the thickness direction of the ultrathin sections), and hence spherical microdomains are clearly resolved. However, in the disordered regions such as shown in Figure 4b, spherical microdomains tend to overlap each other with their centers being displaced each other more or less randomly. When such a 3-dimensional structure is observed on 2-dimensional plane projected perpendicular to the electron beam axis, it is quite natural (and most probable) that the microdomains tend to appear as if they are interconnected, and the interconnected objects have some variations in contrast, which smear the image of the spheres as shown in certain parts of Figure 4b. Judging from the SAXS results shown in Figures 5 and 6, we do not believe that the TEM image of Vector 4113 at 210 °C given in Figure 4b represents a snapshot of "frozen", thermally induced dynamical composition fluctuations in the micelle-free disordered state at temperatures very close to ODT as found in lamella- or cylinder-forming block copolymers, as designated by the D_F structure and elaborated on in ref 37.

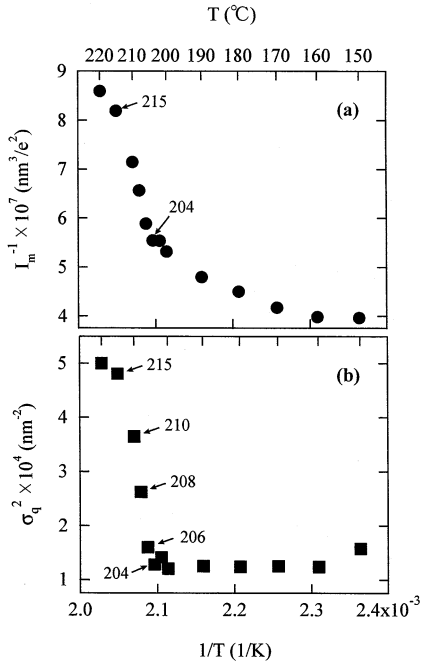

Figure 6. Plots of $1/I_m$ vs $1/T$ and σ_q^2 vs $1/T$ for Vector 4113 in the heating process shown in Figure 5.

Figure 5 shows the SAXS profiles for Vector 4113 measured in situ at various temperatures during the heating process following the thermal protocol described in Figure 1. It should be noted that we rely more on the SAXS results than TEM results for quantitative analyses, because the SAXS results reflect features statistically averaged over a large volume, while TEM highlights features of local structures only. At temperatures equal to and below 208 °C, the scattering maxima arising from the interdomain interference exist at the relative peak positions of $1:\sqrt{2}\sqrt{3}$. These pieces of evidence as well as the volumetric consideration of spheres suggest the existence of the spherical microdomain structure with a body-centered-cubic lattice (bcc-sphere). Above 210 °C, the higher order peaks of $\sqrt{2}$ and $\sqrt{3}$ disappear and turn into a broad shoulder ranging from ca. 0.3 to ca. 0.5 nm^{-1}, suggesting the existence of spherical microdomains with short-range liquidlike order. The above SAXS results indicate that LDOT

takes place at around 208 °C, consistent with the conclusion drawn above from the log G' vs log G'' plots given in Figure 3.

Figure 6 gives plots of the reciprocal of the first-order peak intensity (I_m^{-1}) vs the reciprocal of the absolute temperature (l/T) and plots of square of half-width at half-maximum (σ_q^2) of the first-order peak in SAXS profile for Vector 4113. These two plots show a fairly large discontinuity between 204 and 215 °C. These temperatures are best interpreted as representing the onset and completion of LDOT, respectively. The points at 206 and 208 °C exist in between those at 204 and 215 °C. Thus, we conclude that the disordered-sphere phase and the bcc-sphere phase coexist at temperatures between 204 and 215 °C under the given experimental conditions as indicated by the thermal protocol described in Figure 1. This conclusion is consistent with the conclusion drawn above with reference to Figure 3 that Vector 4113 begins to undergo LDOT above 200 °C. The TEM image given in Figure 4b may suggest the coexistence of the disordered-sphere phase and the bcc-sphere phase at 210 °C. Although it is beyond the scope of this paper to discuss whether the coexistence occurs at thermal equilibrium, the coexistence may occur at thermal equilibrium over a narrow temperature range around T_{LDOT} due to thermal fluctuation effects as elaborated by Fredrickson and Helfand,[15] Hohenberg and Swift,[38] and Hashimoto and co-workers.[37] It is worth noting the following point that is illuminated by comparing the SAXS results in Figure 6 with the rheological behavior in Figure 3 and the TEM image in Figure 4b. The flow of the system at 205−210 °C, as revealed by the log G' vs log G'' plot with a slope of 2 in the terminal region, occurs through flow of ordered grains in the matrix of disordered spheres and flow of the spheres in the disordered matrix phase.

Phase Transitions in Binary Blends of Vector 4113 and Homopolystyrene. Since the T_{DMT} of Vector 4113 lies outside the experimentally accessible temperature range without inducing significant thermal degradation/cross-linking reactions, we have decided to add a low-molecular-weight polystyrene to Vector 4113 in order to bring down transition temperatures below ca. 220 °C. In the present study we employed two polystyrenes, PS-1 having M_n = 900 g/mol and PS-2 having M_n = 1300 g/mol. We obtained log G' vs log G'' plots for 90/10, 80/20, 70/30, and 60/40 Vector 4113/(PS-1) blends and also for 90/10, 80/20, 70/30, 60/40, and 50/50 Vector 4113/(PS-2) blends at various temperatures ranging from 80 to 220 °C using specimens that were annealed at 130 °C for 3 days in a vacuum oven. Further, we also conducted isochronal dynamic temperature sweep experiments at ω = 0.01 rad/s for each blend at temperatures up to 220 °C. For illustration, Figure 7 gives log G' vs log G'' plots for 80/20 Vector 4113/(PS-1) blend at temperatures ranging from 100 to 200 °C. For comparison, also given in Figure 7 are the results of isochronal dynamic temperature sweep experiments at ω = 0.01 rad/s. The results for other blend compositions are not presented here owing to space limitations. Two things are noteworthy in Figure 7. First, we find a threshold temperature at which log G' vs log G'' plots no longer vary, during heating, with temperature, namely 195 °C, which represents the T_{DMT} of this blend. The readers are reminded that such a temperature could not be found in neat Vector 4113 (see Figure 3) Second, the threshold temperature at which the log G' vs log G'' plot

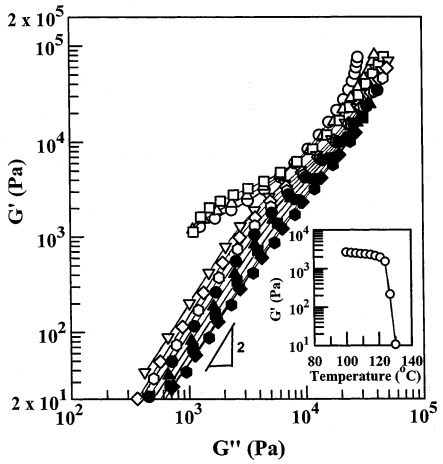

Figure 7. Plots of log G' vs log G'' for 80/20 Vector 4113/(PS-1) blend at various temperatures: (○) 100, (△) 110, (□) 120, (▽) 130, (◇) 140, (⬡) 150, (●) 160, (▲) 170, (■) 180, (▼) 190, (◆) 195, and (⬢) 200 °C. The inset in the lower right corner gives the dependence of G' on temperature during the isochronal dynamic temperature sweep experiment at ω = 0.01 rad/s in the heating cycle. The specimens were annealed at 130 °C for 3 days in a vacuum oven.

begins to exhibit, during heating, a slope of 2 in the terminal region is 130 °C, which represents the T_{LDOT} of the blend. This value is reasonably close (within 5 °C) to the temperature at which G' begins to drop precipitously from the dynamic temperature sweep experiments (see the inset in Figure 7). In our previous papers,[8,9,11] we have shown similar features for other sphere-forming SI diblock and SIS triblock copolymers. The parallel shift of log G' vs log G'' plots in Figure 7 signifies that the 80/20 Vector 4113/(PS-1) blend exhibits liquidlike behavior as discussed above for neat Vector 4113. The log G' vs log G'' plots for other blends are not presented here owing to space limitations.

Using the values of T_{LDOT} and T_{DMT} for each blend, we constructed phase diagrams, given in Figure 8, for Vector 4113/(PS-1) blends and Vector 4113/(PS-2) blends, describing the dependence of T_{LDOT} and T_{DMT} of the respective blends on blend composition, in which DM denotes disordered micelles. Two things are worth noting in Figure 8. The extrapolated values of T_{LDOT} for the respective blends to zero weight fraction of added polystyrene are virtually identical and equal to 205 °C, which is the T_{LDOT} of *neat* Vector 4113 (see Figure 3). More precisely, this T_{LDOT} may signify the onset temperature for LDOT, based on the SAXS results shown in Figure 6. The extrapolated values of T_{DMT} for the respective blends to zero weight fraction of added polystyrene are virtually identical and equal to ca. 260 °C, which represents the T_{DMT} of *neat* Vector 4113 that cannot be determined using neat Vector 4113. In the more rigorous sense, the validity of the assumption should be checked at weight fractions of less than 0.1.

Phase Transitions in SIS-100. Since we could not determine the T_{DMT} of Vector 4113 without inducing significant thermal degradation/cross-linking reactions by heating a specimen above 220 °C, we synthesized a sphere-forming low-molecular-weight SIS triblock copolymer (SIS-100) and investigated whether the block copolymer would undergo both LDOT and DMT within the experimentally accessible temperature range (say below 220 °C). For rheological measurements, the results of which are described below, the solvent-cast specimens of SIS-100 were annealed at 65 °C for 3 days

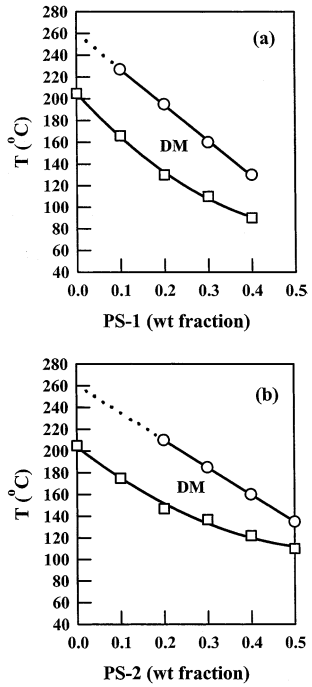

Figure 8. (a) Dependence of T_{LDOT} (□) and T_{DMT} (○) on blend composition for Vector 4113/(PS-1) blends. (b) Dependence of T_{LDOT} (□) and T_{DMT} (○) on blend composition for Vector 4113/(PS-2) blends. DM denotes disordered micelles.

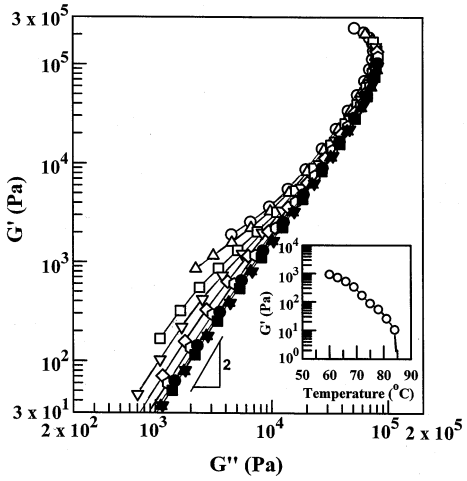

Figure 9. Plots of log G' vs log G'' for SIS-100 at various temperatures: (○) 60, (△) 70, (□) 80, (▽) 85, (◇) 90, (⬡) 95, (●) 100, (▲) 105, (■) 110, and (▼) 115 °C. The inset in the lower right corner gives the dependence of G' on temperature during the isochronal dynamic temperature sweep experiment at $\omega = 0.01$ rad/s in the heating cycle. The specimens were annealed at 65 °C for 3 days in a vacuum oven.

in a vacuum oven. No further annealing was performed after placing a specimen onto the parallel-plate fixture of the rheometer. Figure 9 gives log G' vs log G'' plots for SIS-100 at various temperatures ranging from 60 to 115 °C, and the inset gives the results of the isochronal dynamic temperature sweep experiment at $\omega = 0.01$ rad/s. From the log G' vs log G'' plots given in Figure 9 we determine T_{LDOT} to be ca. 85 °C and T_{DMT} to be ca. 105 °C for SIS-100. Different from Vector 4113, SIS-100 has enabled us to determine both T_{LDOT} and T_{DMT} below 220 °C, for an SIS triblock copolymer. On the other hand, from the isochronal dynamic temperature sweep experiment, the results of which are given in the inset of Figure 9, we observe that G' decreases

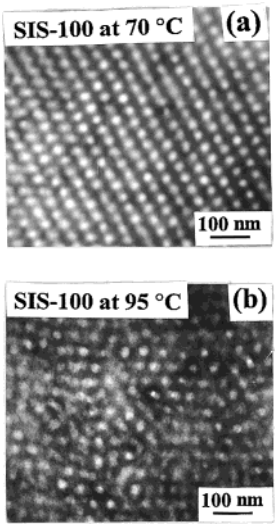

Figure 10. TEM images of SIS-100: (a) after annealing at 70 °C for 4 weeks followed by rapid quenching in ice water; (b) after annealing at 95 °C for 1 week followed by rapid quenching in ice water.

gradually until reaching ca. 85 °C, and thus we cannot identify a temperature at which G' drops precipitously. Such a temperature dependence of G' for SIS-100 is attributable to the very low volume fraction (0.07) of polystyrene block in SIS-100. Thus, we conclude that the isochronal dynamic temperature sweep experiment is not useful to determine the T_{LDOT} of SIS-100.

Figure 10 gives TEM images of SIS-100 specimens that were annealed at 70 °C for 4 weeks and at 95 °C for 1 week, showing clearly that SIS-100 has spherical microdomains in ordered lattice at 70 °C (below T_{LDOT}) and disordered spheres (disordered micelles) at 95 °C (i.e., at $T_{LDOT} \leq T < T_{DMT}$). Such a long period (4 weeks) of annealing was necessary to obtain the TEM images of SIS-100 given in Figure 10, because the volume fraction of polystyrene block in SIS-100 is very low (0.07). In this study we investigated the effect of the duration of annealing on the equilibrium morphology of several compositionally asymmetric SIS triblock copolymers, although the results are not presented here. We found that a longer annealing period was necessary to attain equilibrium morphology as the volume fraction of PS block in an SIS triblock copolymer was decreased. Such an observation is very reasonable, since microdomains may be formed only above a certain critical volume fraction of PS block in an SI diblock or SIS triblock copolymer The slow ordering in this case is clearly due to a small thermodynamic driving force for ordering.

To attain a well-ordered microdomain structure, SIS-100 specimen was annealed at 65 °C for 1 week before the SAXS measurement. Unexpectedly, a weak mechanical perturbation associated with in the process of placing the specimen into our SAXS cell completely destroyed the long-range order of microdomains. Consequently, the SAXS profiles showed only a broad first-order peak and a broad higher order shoulder as shown later in Figure 11 by the profile at 90 °C but no higher order scattering maxima.

To attain the highest possible long-range order in an SIS-100 specimen, we annealed the specimen again at 70 °C for 209 h after the annealed specimen had been placed in the SAXS cell. Figure 11 shows the in-situ SAXS profiles measured at various temperatures in the

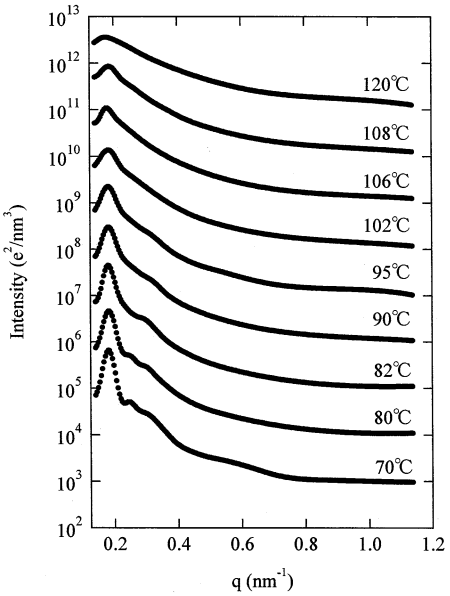

Figure 11. Temperature dependence of desmeared SAXS profiles for SIS-100 in the heating process at various temperatures ranging from 70 to 120 °C. The intensities of the SAXS profiles at 70 °C shown at the bottom of this figure are actually measured values, and the intensities of other SAXS profiles have been shifted up by 1 decade relative to intensities immediately below.

heating process following the thermal protocol described in Figure 1. The following observations are worth noting in Figure 11. Below 80 °C the SAXS profiles show the scattering maxima at 1:$\sqrt{2}$:$\sqrt{3}$ relative to the first-order maximum. These pieces of evidence together with the volumetric considerations of spheres indicate the existence of bcc-sphere. However, at 82 °C the higher-order maxima at $\sqrt{2}$ and $\sqrt{3}$ are broadened and overlap into a broad shoulder, suggesting that LDOT occurs between 80 and 82 °C. Upon increasing temperature further, the shoulder becomes broader and less distinct. Finally, the shoulder becomes almost indistinguishable at temperatures above ca. 106 °C, suggesting that DMT occurs at around 106−108 °C for SIS-100.

Figure 12 gives plots of I_m^{-1} vs $1/T$ plots and plots of σ_q^2 vs $1/T$ for SIS-100. Unlike the results given in Figure 6 for Vector 4113, both I_m^{-1} vs $1/T$ and σ_q^2 vs $1/T$ plots in Figure 12 do *not* show a discontinuity at any particular temperature, which is expected from Figure 11. This observation seems to suggest that the long-range order that existed below T_{LDOT} was subjected to fairly large thermal distortions. However, the T_{DMT} of SIS-100, which is between 106 and 108 °C, is identified by an inflection point in both I_m^{-1} vs $1/T$ and σ_q^2 vs $1/T$ plots given in Figure 12.

Phase Transitions in Binary Blends of SIS-100 and Homopolystyrene. In this study we obtained log G' vs log G'' plots for 90/10, 80/20, 70/30, and 60/40 (SIS-100)/(PS-2) blends at various temperatures ranging from 60 to 130 °C using the specimens that were annealed at 75 °C for 3 days in a vacuum oven. Further, we also conducted isochronal dynamic temperature sweep experiments at $\omega = 0.01$ rad/s for each blend at temperatures up to 130 °C. Those results are not presented here owing to space limitations. From the log G' vs log G'' plots, which showed the same feature as that for neat SIS-100 (see Figure 9), we determined T_{LDOT} and T_{DMT}, which enabled us to construct phase diagrams.

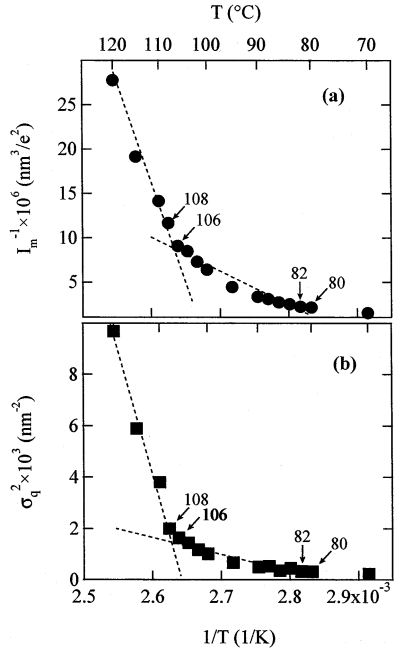

Figure 12. Plots of $1/I_m$ vs $1/T$ and σ_q^2 vs $1/T$ for SIS-100 in the heating process shown in Figure 11.

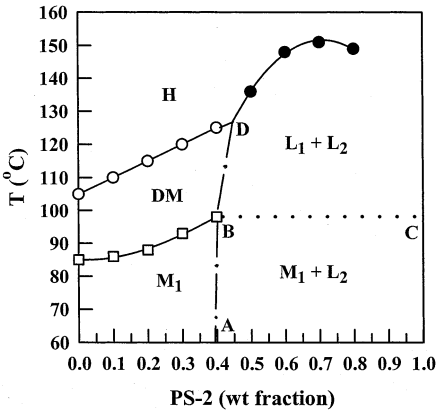

Figure 13. Temperature−composition phase diagram for (SIS-100)/(PS-2) blends, where H denotes the homogeneous phase in which disordered SIS-100 chains and PS-2 chains are mixed on a molecular level, DM denotes disordered micelles, M_1 denotes a mesophase in which the majority of the added PS-2 is solubilized in the PS microdomains of SIS-100, L_1 denotes the macrophase-separated homogeneous phase rich in SIS-100, and L_2 denotes macrophase-separated homogeneous phase rich in PS-2. The symbol ○ denotes T_{DMT}, the symbol □ denotes T_{LDOT}, and the symbol ● denotes cloud point. The dotted line connecting B and C is tentatively drawn to separate the two regions, (M_1 + L_2) and (L_1 + L_2), the experimental determination of which is left for future work, and the dashed−dotted line connecting A and D is drawn simply as a visual aid.

Figure 13 gives a phase diagram for (SIS-100)/(PS-2) blends, where H denotes the homogeneous phase in which disordered SIS-100 chains and PS-2 chains are mixed on a molecular level, DM denotes disordered micelles, and M_1 denotes a mesophase in which the majority of the added PS-2 is solubilized in the PS microdomains of SIS-100, while the rest of PS-2 is dissolved in the matrix and the microdomains seemingly have long-range order. L_1 denotes the macrophase-separated homogeneous phase rich in SIS-100, and L_2 denotes macrophase-separated homogeneous phase rich in PS-2. In Figure 13 the symbol ○ denotes T_{DMT}, the symbol □ denotes T_{LDOT} (onset temperature), and the

symbol ● denotes cloud point. In Figure 13 we observe that the addition of PS-2 to SIS-100 increases both T_{LDOT} and T_{DMT}, opposite to that observed for the addition of PS-1 or PS-2 to Vector 4113 shown in Figure 8. Referring to Figure 13, the region denoted by $(M_1 + L_2)$ represents the two-phase region consisting of the mesophase and macrophase-separated homogeneous phase rich in PS-2, and the region denoted by $(L_1 + L_2)$ represents the two-phase region consisting of the macrophase-separated homogeneous phase rich in SIS-100 and macrophase-separated phase rich in PS-2. The dotted line connecting B and C in Figure 13 is tentatively drawn to separate the two regions, $(M_1 + L_2)$ and $(L_1 + L_2)$, the experimental determination of which is left for future work. The dashed−dotted line connecting A and D in Figure 13 is drawn simply as a visual aid.

It should be mentioned at this juncture that, in constructing a phase diagram for Vector 4113/PS blends, Lee et al.[24] regarded the temperature at which G' begins to drop rapidly in their isochronal dynamic temperature sweep experiments as T_{ODT}. In so doing, they did not investigate the possibility that Vector 4113/PS blends might have disordered micelles at temperatures above the T_{ODT} thus determined. However, log G' vs log G'' plots (see Figure 7) for Vector 4113/PS blends investigated in the present study show that the blends undergo LDOT and DMT; i.e., disordered micelles should exist between T_{LDOT} and T_{DMT} (see Figure 8). Thus, the T_{ODT}'s determined by Lee et al.[24] correspond to the T_{LDOT}'s determined in the present study. We are of the opinion that the phase boundary between the ordered and disordered phases in the phase diagram of ref 24 corresponds to the phase boundary between the ordered phase (M_1) and disordered micelles (DM) in Figure 13. In the phase diagram of ref 24, the phase boundary between the ordered and disordered phases (i.e., their T_{ODT}) goes through a minimum. In offering an explanation on the appearance of a minimum in their phase diagram for the Vector 4113/PS blends, Lee et al. speculated that the chains stretched over a certain range of blend compositions. We think that such a speculation is reasonable *if* the T_{ODT} determined by Lee et al. corresponds to our T_{LDOT}, because a recent study of Vaidya and Han[39] also reported that the phase boundary between the ordered phase (M_1) and disordered micelles (DM) goes through a minimum, while the phase boundary between the homogeneous phase (H) and disordered micelles (DM) does not, in binary blends consisting of a sphere-forming SI diblock copolymer and homopolystyrene. However, the problem lies in that, in obtaining their phase diagrams, Lee et al. conducted SAXS and rheology measurements at temperatures up to 280 °C, which might have exceeded the temperature[32] at which thermal degradation/cross-linking reactions in PI begin to take place (also see Figure 2), granted that thermal degradation/cross-linking reactions in PI may not exactly be reproducible. However, we believe that the experiments in the present study and in ref 39 certainly have reduced the uncertainties associated with the SAXS and rheology measurements of Lee et al.[24] conducted at temperatures up to 280 °C.

4. Concluding Remarks

In this study we synthesized via anionic polymerization a sphere-forming low-molecular-weight SIS triblock copolymer using difunctional initiator and then used this block copolymer to investigate whether it may undergo LDOT and DMT during heating, similar to that observed previously for sphere-forming low-molecular-weight SI diblock copolymers.[11] Indeed we observed that the SIS triblock copolymer undergoes LDOT and DMT, as determined by oscillatory shear rheometry and SAXS. By preparing binary blends consisting of the SIS triblock copolymer and a low-molecular-weight polystyrene, we investigated phase transitions for various blend compositions and then constructed a phase diagram. In so doing, we determined the phase boundary between the homogeneous phase free from micelles or spheres with only thermally induced composition fluctuations and disordered micelles using the T_{DMT} determined from oscillatory shear rheometry, the phase boundary between the homogeneous phase and macrophase-separated phase (i.e., binodal curve) using cloud point measurement, and the phase boundary between the ordered phase and disordered micelles using the T_{LDOT} determined from oscillatory shear rheometry. The phase diagram thus constructed has a region where disordered micelles exist over a certain range of blend compositions.

In this paper we have shown that extreme care is necessary for investigating phase transitions in sphere-forming SIS triblock copolymer using oscillatory shear rheometry or SAXS. Specifically, there are four important things that require careful consideration in this regard. Although they are not necessarily new we wish to point out them below. First, sphere-forming SIS triblock copolymer may undergo LDOT before attaining the micelle-free homogeneous state. The LDOT discussed here is a kind of ODT from bcc-sphere to disordered micelles (or disordered spheres), but the term LDOT describes clearly a physical process and structural change occurring in this ODT. On the other hand, the term ODT for lamellar- or cylinder-forming block copolymers has been used to describe a transition where ODT involves going from ordered lamellae or cylinders to a micelle-free homogeneous phase with only thermally induced composition fluctuations. Whether or not the temperature at which G' in the isochronal dynamic temperature sweep experiment begins to drop precipitously represents T_{ODT} of the type found for lamella- or cylinder-forming block copolymers or T_{LDOT} of the type found for sphere-forming block copolymers must be determined only after investigating the morphology of the specimen, via TEM or SAXS, above such temperature. This is because the isochronal dynamic temperature sweep experiment alone is *not* sufficient to determine whether a *sphere-forming* SIS triblock copolymer might undergo ODT transforming directly into the micelle-free homogeneous state or into the disordered micelles. Second, when conducting isochronal dynamic temperature sweep experiment to investigate phase transition(s) in sphere-forming SIS triblock copolymer, one must employ as low angular frequencies as possible. Third, one must identify the highest measurement temperature for SAXS and oscillatory shear rheometry, below which thermal degradation/cross-linking reactions of specimens may be considered negligible. Fourth, one must give adequate thermal treatment to the specimens prior to SAXS study and oscillatory shear measurement in order to clearly determine LDOT.

Appendix

We wish to clarify some of the statements made in our previous paper,[11] which might be misinterpreted. In ref 11 we stated "the LDT between the ordered

morphology and the disordered micelles is not ODT in the sense of ODT in lamella-forming block copolymer, which is equivalent to DMT in our terminology (Figure 1)." We meant to state "the LDT in highly asymmetric block copolymers from the ordered state of PS spheres into the disordered micelles of spheres must be distinguished from the ODT in lamella-forming block copolymer from the ordered state into the micelle-free homogeneous phase with only thermally-induced composition fluctuations." In other words, the above statement in ref 11 was not meant to imply that ODT in lamella-forming block copolymers is equivalent to DMT in sphere-forming block copolymers. Thus, we suggest that the phrase "which is equivalent to DMT in our terminology (Figure 1)" that appeared in ref 11 be disregarded to avoid confusion.

A brief historical background of the terminologies, ODT, LDT, LDOT, and DMT, would serve a very useful purpose. In 1983, while investigating, via SAXS, the solutions of a sphere-forming polystyrene-*block*-polybutadiene (SB diblock) copolymer in *n*-tetradecane, Hashimoto et al.[14] observed spherical microdomains of PS phase having short-range liquidlike order and then coined for the first time the term lattice disordering temperature, T_{LDT}. They observed that the lattice disordering increased the line profile of the SAXS maximum and also created a discontinuity in the Bragg spacing with increasing temperature.

In 1996 Schwab and Stühn[6] investigated, via SAXS, phase transition in spherical microdomains, during cooling, from a state of liquidlike order to a bcc lattice in highly asymmetric, sphere-forming SI diblock copolymers. They noted that a stable, liquidlike order of the spherical microdomains (disordered micelles) exists at high temperatures. However, they regarded the disordered micelles as part of the disordered state. Adams et al.[4,5] investigated, via rheology and SAXS, phase transition in SI diblock and SIS triblock copolymers and noted the existence of disordered micelles, which they regarded as being part of the disordered phase.

In 1997 Sakamoto et al.[8] investigated, via SAXS and rheology, phase transitions in a cylinder-forming SIS triblock copolymer (Vector 4111) having a 0.183 weight fraction of PS block, in which they observed, during heating, lattice disordering transition (LDT) occurring at temperatures between 210 °C (onset) and 214 °C (completion). They also observed a spherical microdomain structure of PS having a liquidlike short-range order (disordered micelles), which persisted even up to 220 °C, the highest experimental temperature employed, after the block copolymer had undergone an order−order transition (OOT) from cylindrical to spherical microdomains of PS phase at 179−185 °C. Owing to the rather high molecular weight of Vector 4111, in their study Sakamoto et al. could not determine the temperature at which disordered micelles might transform into the micelle-free state having thermal composition fluctuations. Thus, in 2000 Han et al.[11] synthesized highly asymmetric low-molecular-weight SI diblock copolymers, enabling them to determine, via SAXS and rheology, both transition temperatures, one at which spherical microdomains in bcc lattice transform into disordered micelles with short-range order and another at which disordered micelles transform into a micelle-free state having thermal composition fluctuations. In so doing, the authors coined the term LDOT describing the lower transition temperature and the term DMT describing the upper transition temperature for the two transition temperatures observed in the low-molecular-weight SI diblock copolymers.

References and Notes

(1) Hashimoto, T. In *Thermoplastic Elastomers*; Holden, G., Legge, N. R., Quirk, R., Schroeder, H. E., Eds.; Hanser: Munich, 1996; Chapter 15A.
(2) Leibler, L. *Macromolecules* **1980**, *13*, 1602.
(3) Helfand, E.; Wasserman, Z. R. In *Developments in Block Copolymers*; Goodman, I., Ed.; Applied Science: New York, 1982; Chapter 4.
(4) Adams, J. L.; Graessley, W. W.; Register, R. A. *Macromolecules* **1994**, *27*, 6026.
(5) Adams, J. L.; Quiram, D. J.; Graessley, W. W.; Register, R. A.; Marchand, G. R. *Macromolecules* **1996**, *29*, 2929.
(6) Schwab, M.; Stühn, B. *Phys. Rev. Lett.* **1996**, *76*, 924.
(7) Schwab, M.; Stühn, B. *Colloid Polym. Sci.* **1997**, *275*, 341.
(8) Sakamoto, N.; Hashimoto, T.; Han, C. D.; Kim, D.; Vaidya, N. Y. *Macromolecules* **1997**, *30*, 1621.
(9) Sakamoto, N.; Hashimoto, T.; Han, C. D.; Kim, D.; Vaidya, N. Y. *Macromolecules* **1997**, *30*, 5321.
(10) Sakamoto, N.; Hashimoto, T. *Macromolecules* **1998**, *31*, 8493.
(11) Han, C. D.; Vaidya, N. Y.; Kim, D.; Shin, G.; Yamaguchi, D.; Hashimoto, T. *Macromolecules* **2000**, *33*, 3767.
(12) Kim, J. K.; Lee, H. H.; Sakurai, S.; Aida, S.; Masamoto, J.; Nomura, S.; Kitagawa, Y.; Suda, Y. *Macromolecules* **1999**, *32*, 6707.
(13) We wish to mention that in some of our earlier studies[8−10] we defined DMT as simply order-to-disorder transition (ODT) under a clear identification of its physical process, on the basis of the entropy change associated with DMT. This definition based on the earlier work of ref 14 was generally accepted and thought to be reasonable at that time in the early 1980s, because the microphase separation (or micellization) and microphase dissolution (or demicellization, respectively), were considered to be equivalent to ordering and disordering processes. However, to avoid confusion of this definition of ODT with the concept of ODT later introduced in a paper by Fredrickson and Helfand,[15] in our recent paper[11] we redefined our earlier definition of ODT as DMT.
(14) Hashimoto, T.; Shibayama, M.; Kawai, H.; Watanabe, H.; Kotaka, T. *Macromolecules* **1983**, *16*, 361.
(15) Fredrickson, G. H.; Helfand, E. *J. Chem. Phys.* **1987**, *87*, 697.
(16) Kinning, D. J.; Winey, K. I.; Thomas, E. L. *Macromolecules* **1988**, *21*, 3502.
(17) Kinning, D. J.; Thomas, E. L. *J. Chem. Phys.* **1988**, *90*, 5806.
(18) Winey, K. I.; Thomas, E. L.; Fetters, L. J. *Macromolecules* **1992**, *25*, 2645.
(19) Dormidontova, E. E.; Lodge, T. P. *Macromolecules* **2001**, *34*, 9143.
(20) Semenov, A. N. *Sov. Phys. JETP* **1985**, *61*, 733.
(21) Semenov, A. N. *Macromolecules* **1989**, *22*, 2849.
(22) Matsen, M. W.; Bates, F. S. *Macromolecules* **1996**, *29*, 1091.
(23) Matsen, M. W.; Bates, F. S. *J. Chem. Phys.* **1997**, *106*, 2436.
(24) Lee, S.-H.; Char, K.; Kim, G. *Macromolecules* **2000**, *33*, 7072.
(25) (a) Tung, L. H.; Lo, Y. S. *Macromolecules* **1994**, *27*, 2219. (b) Lo, G. Y.; Ottrerbacher, E. W.; Gatzke, A. L.; Tung, L. H. *Macromolecules* **1994**, *27*, 2233.
(26) Broske, A. D.; Huang, T. L.; Allen, R. D.; Hoover, J. M.; MaGrath, J. E. In *Recent Advances in Anionic Polymerization;* Hogen-Esch, T. E., Smid, J., Eds.; Elsevier Science: New York, 1987; p 363.
(27) Lee, B. Anionic Polymerization Chemistry of 1,1-Diphenylethylene and Its Analogs. Doctoral Dissertation, The University of Akron, Akron OH, 1991.
(28) Hashimoto, T.; Suehiro, S.; Shibayama, M.; Saijo, K.; Kawai, H. *Polym. J.* **1981**, *13*, 501.
(29) Suehiro, S.; Saijo, K.; Ohta, Y.; Hashimoto, T.; Kawai, H. *Anal. Chim. Acta* **1986**, *189*, 41.
(30) Fujimura, M.; Hashimoto, T.; Kawai, H. *Mem. Fac. Eng., Kyoto Univ.* **1981**, *43*, 224.
(31) Hendricks, R. W. *J. Appl. Crystallogr.* **1972**; *5*, 315.
(32) Han, J. H.; Feng, D.; Choi-Feng, C.; Han, C. D. *Polymer* **1995**, *36*, 155.
(33) (a) Han, C. D.; Kim, J. *J. Polym. Sci., Polym. Phys. Ed.* **1987**, *25*, 1741. (b) Han, C. D.; Kim, J.; Kim, J. K. *Macromolecules* **1989**, *22*, 383. (c) Han, C. D.; Baek, D. M.; Kim, J. K. *Macromolecules* **1990**, *23*, 561.
(34) (a) Gouinlock, E. V.; Porter, R. S. *Polym. Eng. Sci.* **1977**, *17*, 534. (b) Chung, C. I.; Lin, M. I. *J. Polym. Sci., Polym. Phys.*

Ed. **1978**, *16*, 545. (c) Widmaier, J. M.; Meyer, G. C. *J. Polym. Sci., Polym. Phys. Ed.* **1980**, *18*, 217.
(35) Rosedale, J. H.; Bates, F. S. *Macromolecules* **1990**, *23*, 2329.
(36) Han, C. D.; Baek, D. M.; Kim, J. K.; Ogawa, T.; Sakamoto, N.; Hashimoto, T. *Macromolecules* **1995**, *28*, 5043 and references therein.
(37) (a) Sakamoto, N.; Hashimoto, T. *Macromolecules* **1995**, *28*, 6825. (b) Sakamoto, N.; Hashimoto, T. *Macromolecules* **1998**, *31*, 3815. (c) Hashimoto, T.; Koga, T.; Koga, T.; Sakamoto, N. In *Physics of Complex Fluids*; Yonezawa, F., Tsuji, K., Kaji, K., Doi, M., Fujiwara, T., Eds.; World Scientific: Singapore, 1998; p 29ff. (d) Koga, T.; Koga, T.; Hashimoto, T. *J. Chem. Phys.* **1999**, *110*, 11076. (e) Hashimoto, T. *Macromol. Symp.* **2001**, *174*, 69.
(38) Hohenberg, G. H.; Swift, J. B. *Phys. Rev. E* **1995**, *52*, 1828.
(39) Vaidya, N. Y.; Han, C. D. *Polymer* **2002**, *43*, 3047.

MA020684Q